Chemical kinetic aspects of hyperpolarization buildup and decay revealed via side-arm para-hydrogenation of vinylated fatty acid precursors

Erik Van Dyke, Maksim Tsukanov, Bea Bliemel, Danila A. Barskiy, Alexander Pines
University of California – Berkeley, College of Chemistry, QB3, Berkeley CA 94720 USA

Introduction

Fatty acids (FAs) are known to be a convenient target for diagnosing and tracking progression of metabolic syndrome, some forms of cancer, and bowel disorders [1]. We selected vinylated precursors of FAs to assess their ability to undergo side-arm hydrogenation (SAH) [2-3]. We examined the kinetics of hyperpolarization buildup and decay for the products of para-hydrogenation of vinylated FA precursors containing aliphatic, unbranching moieties of 2, 4, 5, 10, and 12 carbons in length at various pressures, reagent concentrations, and parahydrogen bubbling times using a Nanalysis benchtop NMR spectrometer (60 MHz). We elaborated a simple analytical model considering dissolution of para-hydrogen gas in the solvent and hydrogenation of the reagent. We derive an equation describing the product formation as a function of time and reaction parameters (equation 8).

Methods

- All measurements were taken using a benchtop NMR spectrometer (Nanalysis NMRPro60, 1.4 T), and a solvent system of 90% chloroform-*d* and 10% methanol-d_4
- Solutions were prepared with 25 mM, 50 mM, or 100 mM vinylated FA and 1 mM, 2.5 mM, or 5 mM [1,4-bis(diphenylphosphino)butane] (1,5-cyclooctadiene) rhodium(I) tetrafluoroborate ([Rh])
- Each sample contained 0.5 mL of solution
- Para-hydrogen pressure was set using an inline pressure regulator at 1 atm, 4.4 atm, 7.8 atm
- PTFE tubing connected sample tubes to a p-H_2 generator which cools H_2 to 20 K over an Fe(OH) catalyst, theoretically producing 100% p-H_2.
- Each sample was bubbled using a manual or automatic valve at constant pressure and a flow rate of 60 scc/m set by a mass flow controller
- No transfer of polarization to heteronuclei, proton signal measured directly.
- Digitally controlled solenoid valve coupled to Arduino and a user-friendly GUI allowed for precise bubbling times

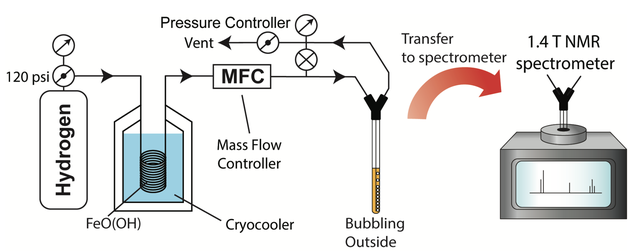

Figure 1. Diagram of the setup used for bubbling the sample with parahydrogen based on the ALTADENA method. Hydrogen was flowed through a cryocooler to cool the hydrogen to a temperature of around 20 K to theoretically achieve 100% parahydrogen. The flow of parahydrogen used for bubbling was controlled using a mass flow controller. The circle with crossed lines represents a bypass valve and the circle with a single line represents the pressure regulator for the gas flow setup. Bubbling parahydrogen in the sample was done outside the spectrometer at Earth's field. After the bubbling was complete, the sample was instantaneously transferred into the 1.4T NMR spectrometer to get a spectrum. Late spectra were obtained using the PASADENA method by bubbling inside the spectrometer.

- ALTADENA experiments bubbled using a 1/16" OD capillary.
- Homogeneity was improved by using a thinner capillary in PASADENA experiments.

Mapping buildup and decay of hyperpolarization

- We attempt to explain the behavior seen in figure 2 by using the system of equations outlined below.
- Dissolution and evaporation of hydrogen governed by rate constants k_+ and k_-
  - $\mathbf{H_2^g} \underset{k_-}{\overset{k_+}{\longleftrightarrow}} \mathbf{H_2^l}$
- Hydrogenation occurs as a first order reaction provided substrate (R) is the only limiting component.
  - $\mathbf{H_2^l + R \xrightarrow{k_{H_2}} P}$
- If para-hydrogen is used, then hydrogenation creates a hyperpolarized population of substrate molecules (P^*)
  - $\mathbf{P^* \xrightarrow{T_1} 0}$
- Solving differential rate equations for P^* yields the equation:
  - $[\boldsymbol{P^*}](\boldsymbol{t}) = \boldsymbol{\lambda \eta k_{H_2}[H_2]_0 \frac{\tau T_1}{\tau - T_1}\left(e^{-\frac{t}{\tau}} - e^{-\frac{t}{T_1}}\right)}$
- With τ representing the effective reaction time
  - $\boldsymbol{\tau^{-1} = k_+[H_2^g]}$
- Slow dissolution of hydrogen causes deviation from analytical model

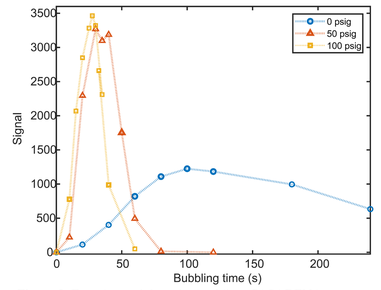

Figure 2. Experimental data obtained from PASADENA experiments at 1.4 T with 100 mM vinyl butyrate and 5 mM Rh(COD). Each point represents signal obtained from a fresh sample bubbled with p-H_2.

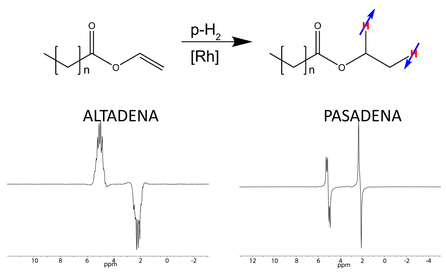

Figure 3. Representative spectra from PHIP experiments of vinyl laurate (left) which was para-hydrogenated at Earth's field and vinyl butyrate (right) para-hydrogenated at 1.4 T.

PHIP Kinetics of Vinylated Fatty Acids

- We conducted kinetic studies for several short to medium chain fatty acids including vinyl acetate, butyrate, valerate, and decanoate.
- Fitting of the butyrate and decanoate data yielded similar values, yet there is room for improvement.
- The fit could be further optimized through reworking the model or taking additional timepoints to establish error bounds.

Figure 4. Experimentally obtained data fitted using equation 8, Each sample was bubbled succesively for 10 sec intervals before a spectra was taken.

Modeling hydrogenation of vinylated fatty acids

- Comparison of models fit to normalized conversion data at 50 mM vinyl laurate and 5 mM Rh(COD).
- The left figure is fitted using a simple first order kinetic model
  - $[P] = [R]_0(1 - e^{-k_{H_2}[R]_0 t})$,
- The right figure is fitted according to our quasi-steady state approximation taking the rate of hydrogen dissolution into account.
  - $t = \frac{[R]_0 - [R]}{k_+[H_2^g]} - \frac{1}{k_{H_2}} \ln \frac{[R]}{[R]_0}$
- Quasi steady state assumptions serve as the basis for analytical models of the overall system kinetics.

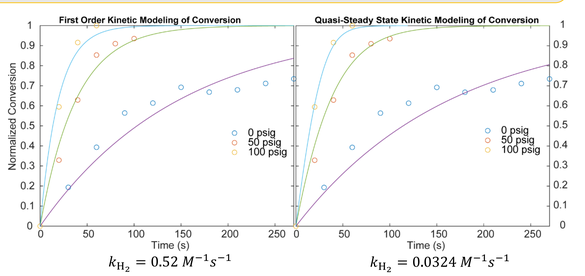

Figure 5. Conversion of vinyl laurate (n = 12) by thermal hydrogen at different pressures. Fitting with two different models yields rate constants that may be used to model the buildup and decay of PHIP.

Quasi-steady state assumptions

$$\frac{d[\mathbf{H_2^g}]}{dt} = -k_+[\mathbf{H_2^g}] + k_-[\mathbf{H_2^l}] \approx 0 \quad (9)$$

$$\frac{d[\mathbf{H_2^l}]}{dt} = k_+[\mathbf{H_2^g}] - k_-[\mathbf{H_2^l}] - k_{\mathbf{H_2}}[\mathbf{H_2^l}][\mathbf{R}] \approx 0 \quad (10)$$

Optimizing catalyst strength

- Catalyst concentrations of 1, 2.5, and 5 mM were tested
- Signal strength follows predictable trend increasing with greater catalyst and substrate concentrations
- Preliminary results show enhancement greatest at 50 mM substrate with 5 mM catalyst.

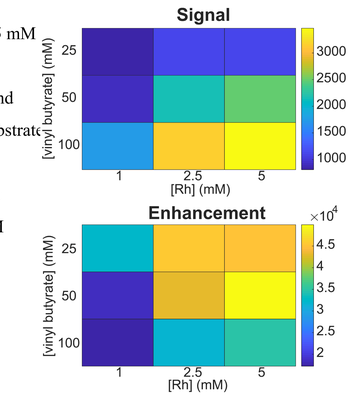

Figure 6. 2D map showing the contrast between maximum observable signal and actual enhancement of substrate at 7.8 atm.

PASADENA and ALTADENA mixing at 1 atm

- Some samples were hydrogenated directly at high field inside the spectrometer. Of these samples, those taken at low pressure showed unexpected shapes.
- The spectra we observed appeared to be a mixture of PASADENA and ALTADENA, which could occur if the samples existed in a mixture of high and low magnetic fields.
- This behavior was only observed in samples para-hydrogenated at 1 atm.

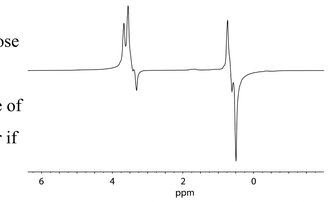

Figure 7. Spectrum of 100 mM vinyl butyrate with 5 mM Rh(COD) after undergoing 60 seconds of para-hydrogenation at 1 atm while inside the bore of a 1.4 T spectrometer.

Conclusions

- Modeling of the PHIP kinetics yielded coherent values for of vinyl laurate however further optimization needs to be done to validate these results.
- Ethyl laurate has already been studied as a drug-delivery agent (13), so cleavage of the hydrogenated moiety could potentially be omitted in *in-vivo* studies.
- One advantage of using shorter chain fatty acids is their higher partition coefficient in water, allowing higher concentration in plasma.
- Further development of modeling the behavior of hyperpolarization in solution could support *in vivo* work.
- These experiments could be used in a teaching setting to demonstrate kinetics and familiarize students with hyperpolarization in a cost-effective manner.

References

1. Rubin, S. M. et al., 2002, *JMB, 322(2), 425–440.* doi:10.1016/s0022-2836(02)00739-8
2. Li, L. et al., 2002, *Int. J. Pharm., 237(1-2), 77–85.* doi:10.1016/s0378-5173(02)00029-7
3.Sriram, R. et al., 2014, *eMagRes, 311-324.* doi:10.1002/9780470034590.emrstm1253
4.Eills, J. et al, 2019, *JACS,* doi:10.1021/jacs.9b10094
5.Cavallari, E. et al., 2020, *Frontiers in Oncology,10.* doi:10.3389/fonc.2020.00497
6.Besten, G. D. et al., 2013, *JLR,* 54, 2325-2340.
7.Bergman, E. et al., 1965, *Biochem. J,* 97(1), 53–58. doi:10.1042/bj0970053
8.Berit, M. et al, 2006 Medium-chain triglycerides. *International Dairy Journal.* 16(11), 1374-1382.
9.Bhattacharya, A. A. et al., 2000, *JMB,* 303(5), 721-732
10.Kovtunov, K. V. et al., 2019, *Chem. Asian J, 13(15), 1857–1871.* doi:10.1002/asia.201800551
11.Reineri, F. et al., 2015, *Nat. Commun., 6(1).* doi:10.1038/ncomms6858
12.Pravica, M. G. et al., 1988, *Chem. Phys. Lett.,* 145(4), 255–258. doi:10.1016/0009-2614(88)80002-2
13.Maxted, E. B. et al., 1981 Solubility Data Series: Hydrogen and Deuterium *IUPAC SDS Vol 5/6 Analytical Chemistry Division Commission on Solubility Data.*
14.Li, L. et al., 2002, *Int. J. Pharm., 237(1-2), 77–85.* doi:10.1016/s0378-5173(02)00029-7